Kinetics of the end of range damage dissolution in flash-assist rapid thermal processing

R. A. Camillo-Castillo[a)]
Department of Materials Science and Engineering, University of Florida, Gainesville, Florida 32611-6130

Mark E. Law
Department of Electrical and Computer Engineering, University of Florida, Gainesville, Florida 32611-6130

Kevin S. Jones
Department of Materials Science and Engineering, University of Florida, Gainesville, Florida 32611-6130

Ljubo Radic
Department of Electrical and Computer Engineering, University of Florida, Gainesville, Florida 32611-6130

R. Lindsay
Infineon Technologies AG, Hopewell Junction, New York 12533

S. McCoy
Mattson Technology, Vancouver, British Columbia, V6P 6T7 Canada

(Received 29 November 2005; accepted 4 April 2006; published online 5 June 2006)

This study investigates the effectiveness of flash-assist rapid thermal processing in dissolving the end of range damage inherent to preamorphizing implants. A series of silicon wafers is preamorphized with a Ge implant and subsequently implanted with B. The wafers are then subjected to a flash anneal, a rapid thermal anneal, or both annealing processes. The flash anneal results in higher defect densities and trapped interstitials than the rapid thermal anneal. Defect dissolution has been previously reported to have an activation energy between 4 and 5 eV. This work demonstrates that the defect dissolution during flash-assist rapid thermal processing is mediated by a 2.2 ± 0.05 eV activation energy. © *2006 American Institute of Physics*.
[DOI: 10.1063/1.2201043]

One of the main challenges to the continued scaling of metal-oxide-semiconductor (MOS) transistor technology is the attainment of low-resistance, ultrashallow layers. Current MOS process flows employ ion implantation technology for amorphization and subsequent dopant introduction into the silicon crystal lattice. The preamorphization implant serves to distort the crystal structure such that there is reduced channeling of the dopant atoms down the interstitial rows, thereby allowing for shallow junction formation. Although the ion implantation process offers a number of advantages, the inherent damage to the crystal structure must be repaired, since it contributes to the mobility degradation in final device structures.[1] Lattice repair is achieved by the application of an anneal. Regrowth of the amorphous layers via annealing results in the formation of end of range (EOR) defects beyond the amorphous-crystalline interface.[2] These defects are known to exist as small interstitial clusters of a few atoms, 311-type defects, and dislocation loops. Their thermal evolution has been extensively studied[3–6] and it is widely accepted that submicroscopic interstitial clusters (SMICs) are precursors for the nucleation of {311}-type defects. The unfaulting of the {311}-type defects results in the formation of dislocation loops.[7,8]

The fundamental difference between flash-assist rapid thermal processing (RTP) and rapid thermal annealing (RTA) is that the flash pulse heats only the near surface region of the wafer surface, such that the heat generated can be efficiently conducted away from the surface by the cooler layers on the back side of the wafer, after the flash. This enables extremely high heating and cooling rates on the order of 10^6 °C s^{-1}. In contrast, a RTA results in the entire wafer being heated to the anneal temperature, at much lower heating rates (~ 150 °C s^{-1}) and cooling rates (<100 °C s^{-1}). Hence, the thermal budget imparted to the wafer is significantly higher than that of the flash process. This work explores whether the reduced thermal budget of flash-assist RTP and the differences in thermal gradient into the wafer are as effective as the currently employed RTA in eliminating the EOR damage.

200 mm 12 Ω cm (100) *n*-type Czochralski (CZ) grown silicon wafers were preamorphized with either a 30 or 8 keV germanium ion implant at a dose of 1×10^{15} cm^{-2}, resulting in the formation of continuous amorphous layers 50 or 20 nm deep, respectively. Boron was subsequently implanted at 1 keV, at a dose of 1×10^{15} cm^{-2} with a ~4 nm projected range. All implants were performed in deceleration mode on an Applied Materials XR80 leap implanter at a twist/tilt of 27°/7°. The wafers were then subjected to one of three annealing schemes—flash-assist RTP, RTA, or a combination of both flash-assist RTP and RTA. The flash-assist RTP anneal was performed at Vortek Technologies in Vancouver, Canada and consisted of a ramp up to an intermediate temperature (iRTP) of 700 °C at a rate of 150 °C s^{-1}. The flash anneal (fRTP) which arises by discharging capacitor banks into flash lamps, produced a pulse with a full width at half maximum (FWHM) of ~0.85–0.9 ms, enabling ramp rates on the order of 10^6 °C s^{-1} from the iRTP to temperatures of 1000, 1100, 1200, and 1300 °C. An AG Associates 210 rapid ther-

[a)]Electronic mail: rcamillo@ufl.edu

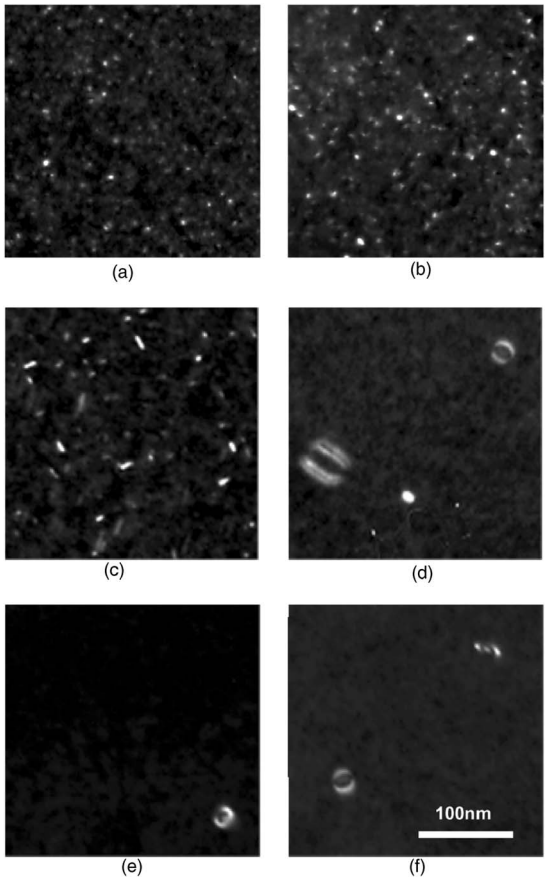

FIG. 1. WBDF PTEM images taken at g_{220} diffraction conditions of the end of range damage for the following anneal conditions: (a) 700 °C iRTP, 1000 °C fRTP, (b) 700 °C iRTP, 1100 °C fRTP, (c) 700 °C iRTP, 1200 °C fRTP, (d) 700 °C iRTP, 1300 °C fRTP, (e) 700 °C iRTP, 1100 °C fRTP +950 °C RTA, and (f) 950 °C RTA only.

mal annealer was utilized for the RTA, which comprised a ramp to a soak temperature of 600 °C at a rate of 100 °C s^{-1}. The temperature was held constant for 10 s prior to ramping up to the desired spike temperature of 950 °C at the same rate. All anneals were performed under nitrogen ambient. Plan-view transmission electron microscopy (PTEM) was utilized to examine the annealed silicon microstructure. A JEOL 200CX microscope was employed in the data acquisition operating at an accelerating voltage of 200 keV. PTEM samples were prepared by standard HF/HNO_3 back side etching techniques and the extended defects were imaged under weak beam dark field (WBDF) g_{220} conditions. Defect densities and trapped interstitial concentrations were determined by the quantification technique of Bharatan *et al.*[9]

Figure 1 depicts the WBDF PTEM images obtained for the EOR damage observed for the flash-assist RTP. Examination of the damage formed by the 30 keV Ge preamorphizing implant (PAI) reveals the presence of small dotlike interstitial clusters of very high density throughout the microstructure, immediately after the 700 °C iRTP anneal. On application of a 1000 °C fRTP virtually no change in microstructure could be discerned. However, as the flash temperature is increased to 1100 °C, some signs of coarsening become apparent. This trend is sustained as the fRTP temperature is raised to 1200 and 1300 °C, in which cases the defects are observed to coarsen into {311}-type structures and dislocation loops. Analysis of the damage for the 8 keV

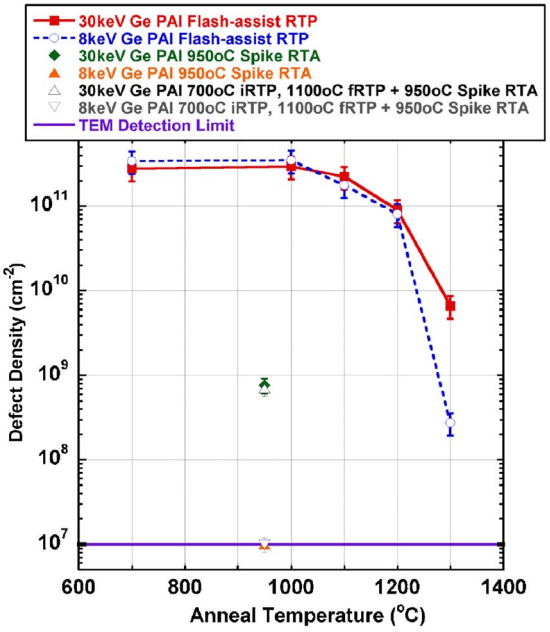

FIG. 2. (Color online) Defect density as a function of anneal temperature for 30 and 8 keV Ge PAIs.

Ge PAI demonstrates very similar evolution behavior. This defect evolution is typical of an Ostwald ripening process in which the larger defects grow at the expense of the smaller ones and demonstrates that increasing the fRTP temperature is capable of evolving the EOR damage inherent to Ge PAIs. This is beneficial from a junction leakage perspective.

In an effort to compare the effectiveness of the flash-assist RTP in reducing the damage formed by Ge PAIs to the commonly used RTA in the complementary metal-oxide-semiconductor (CMOS) process flow, some wafers were subjected to a 950 °C spike RTA. Presumably, the RTA was sufficient to dissolve the EOR damage for the 8 keV Ge PAI, since no defects are observed within the resolution limits of the JEOL 200CX TEM. In the case of the 30 keV Ge PAI, however, small dislocation loops of relatively low density can be seen scattered throughout the microstructure. The WBDF PTEM images for the 30 keV Ge PAIs are shown in Fig. 1. Visual inspection of the images obtained for these two annealing schemes hints at the fact that the defect densities obtained for the RTA process are less than that observed for the flash-assist RTP. This is quite plausible, since the thermal

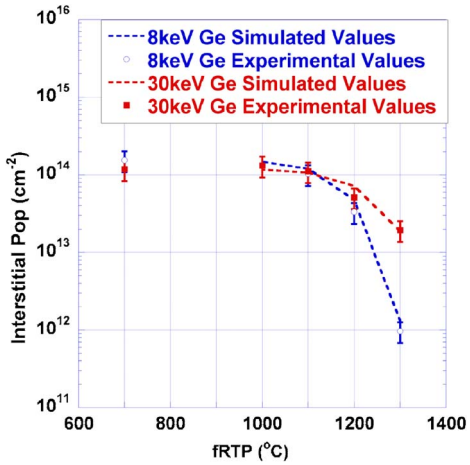

FIG. 3. (Color online) Experimental and simulated trapped interstitials as a function of the flash anneal temperature for 30 and 8 keV Ge PAIs.

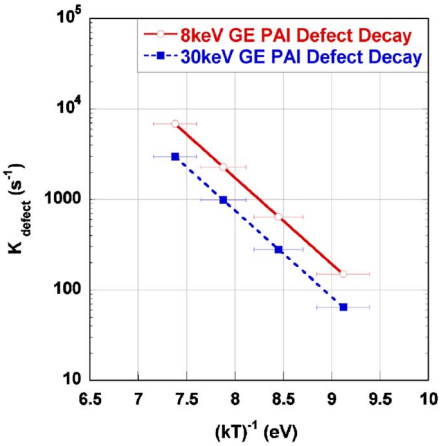

FIG. 4. (Color online) Arrhenius plot of the time constant derived for defect decay extracted from the simulated experimental data, indicating an activation energy E_a of 2.2±0.05 eV for dissolution.

budget applied to the wafer for a RTA is larger than that for a flash-assist RTP, in which the time frame of the anneal is on the order of milliseconds. The WBDF PTEM images of both the 30 keV Ge PAI samples which were annealed at a fRTP temperature of 1100 °C and subsequently subjected to the 950 °C spike RTA can be seen in Fig. 1. There is no apparent difference in the microstructure between the samples which were processed by flash-assist RTP prior to the RTA and those which were processed by the RTA alone.

Figure 2 depicts a plot of the EOR defect density as a function of the anneal temperature for samples which were subjected to the flash-assist RTP and the RTA. The quantification verifies that the defects are undergoing coarsening as the fRTP is increased from 1000 to 1300 °C, since the defect density is observed to decrease exponentially with a concomitant increase in size. There is no noticeable difference in the defect density between the 30 and 8 keV Ge PAIs until the 1300 °C fRTP is attained, at which the densities differ by an order of magnitude. Additionally, the spike RTA results in much lower defect densities than their flash counterparts, confirming that the RTA may in fact be more effective at evolving the EOR damage. It is intriguing that the defect densities for the samples which were processed by flash-assist RTP prior to the RTA and those which were processed by the RTA alone coincide. This detail strongly suggests that during the flash-assist RTP the defects are in the early stages of growth and the additional thermal budget imparted to the wafer during the RTA affects further evolution.

The trapped interstitial population in the extended defects as a function of fRTP temperature is shown in Fig. 3. As the fRTP temperature is increased above 1000 °C, the number of trapped interstitials decreases for both Ge PAIs in an apparent exponential fashion. This behavior coincides with the simultaneous decay in defect density observed and may therefore be indicative of defect dissolution. The numbers of trapped interstitials appear to be independent of Ge PAI energy, except at 1300 °C fRTP, where the interstitial count of the 30 keV Ge PAI exceeds that of the 8 keV Ge PAI by an order of magnitude. This is reasonable as it is expected that the 30 keV Ge PAI would produce a larger number of recoil atoms from the amorphous region into the crystalline region just below it. Hence, there should be more interstitials in the EOR region and therefore the number of trapped interstitials is expected to be greater.

The rate of change of extended defects in the system is a function of both their growth and dissolution. Since the experimental data indicate that the system may be in the dissolution regime, it is assumed that the growth of defects is not significant. Hence, in accordance with kinetic theory the decay rate of the extended defects can be approximated by

$$\frac{\partial C_{\text{interstitials}}}{\partial t} = -\frac{C_{\text{interstitials}}}{\tau}, \tag{1}$$

where $C_{\text{interstitials}}$ is the concentration of trapped interstitials (cm^{-2}), t(s) is anneal time, and $\tau(s)$ is the defect lifetime, which is related to the anneal temperature $T(K)$ by the Arrhenius expression which includes an activation energy E_a,

$$\tau = \tau_0 \exp\left(\frac{E_a}{kT}\right). \tag{2}$$

The process simulator FLOOPS (Ref. 10) was utilized to fit the experimental data. The simulation incorporated the temperature-time variation for each anneal, thus enabling τ to be accurately accounted for in time as the temperature was varied. This facilitated a precise integration of the trapped interstitials with time. Figure 3 demonstrates the close agreement between the simulations and the experimental data. The decay rates derived from the fits of the experimental trapped interstitial populations are illustrated in Fig. 4. In both cases the variation of the decay rate with the inverse of kT generates straight lines which are parallel to each other, indicative of the same activation energy for defect dissolution. An activation energy E_a of 2.2±0.05 eV was determined for dissolution of the extended defects during the flash-assist RTP for these sets of experimental data, with preexponential factors K_0 of 3.3×10^{10} and 7.7×10^{10} s^{-1}, respectively, for the 30 and 8 keV Ge PAIs.

In conclusion, the flash-assist RTP has been shown to significantly dissolve the EOR damage associated with PAIs. The dissolution kinetics that governs this process are mediated by an activation energy of 2.2±0.05 eV. This kinetics differs significantly from previous reports of defect dissolution,[6,11] indicative of an inherent difference in the defect dissolution via flash-assist RTPs. Additionally, the extremely short anneal times employed in the flash-assist process may be probing the initial stages of the defect evolution. It is apparent that a RTA may be more effective in eradicating the EOR damage formed by PAIs.

[1]International Technology Roadmap for Semiconductors, available at http://public.itrs.net/
[2]K. S. Jones, S. Prussin, and E. R. Weber, Appl. Phys. A: Mater. Sci. Process. **45**, 1 (1998).
[3]S. Coffa, S. Libertino, and C. Spinella, Appl. Phys. Lett. **76**, 321 (2000).
[4]S. Libertino, J. L. Benton, S. Coffa, and D. J. Eaglesham, Mater. Res. Soc. Symp. Proc. **504**, 3 (1998).
[5]J. L. Benton, S. Libertino, P. Kringoi, D. J. Eaglesham, J. M. Poate, and S. Coffa, J. Appl. Phys. **82**, 120 (1997).
[6]P. A. Stolk, H.-J. Gossmann, D. J. Eaglesham, D. C. Jacobson, C. S. Rafferty, G. H. Gilmer, M. Jaraíz, J. M. Poate, H. S. Luftman, and T. E. Haynes, J. Appl. Phys. **81**, 9 (1997).
[7]D. J. Eaglesham, P. A. Stolk, H.-J. Gossmann, and J. M. Poate, Appl. Phys. Lett. **65**, 18 (1994).
[8]J. Li and K. S. Jones, Appl. Phys. Lett. **73**, 25 (1998).
[9]S. Bharatan, J. Desrouches, and K. S. Jones, *Materials and Process Characterization of Ion Implantation* (Ion Beam, Austin, TX, 1997), Vol. 4, p. 222.
[10]M. E. Law, SWAMP Center, Electrical and Computer Engineering Department, University of Florida.
[11]T. E. Siedel, D. J. Lischner, C. S. Pai, R. V. Knoell, D. M. Maher, and D. C. Jacobson, Nucl. Instrum. Methods Phys. Res. B **7/8**, 251 (1985).